








Article

# Energy Recovery via Thermal Gasification from Waste Insulation Electrical Cables (WIEC)

Roberta Mota-Panizio <sup>1,2,\*</sup>, Manuel Jesús Hermoso-Orzáez <sup>3,\*</sup>, Luís Carmo-Calado <sup>1</sup>,  
Victor Arruda Ferraz de Campos <sup>4</sup>, José Luz Silveira <sup>4</sup>, Maria Margarida Gonçalves <sup>2</sup> and  
Paulo Brito <sup>5</sup>

<sup>1</sup> IPPortalegre—Polytechnic Institute of Portalegre, 7300-555 Portalegre, Portugal; luis.calado@ippportalegre.pt

<sup>2</sup> Department of Science and Technology of Biomass, Faculty of Science and Technology, METRICs—Mechanical Engineering and Resource Sustainability Center, Universidade NOVA de Lisboa, 2829-516 Caparica, Portugal; mmpg@fct.unl.pt

<sup>3</sup> Department of Graphic Engineering Design and Projects, Universidad de Jaen, 23071 Jaen, Spain

<sup>4</sup> Department of Energy, Faculty of Engineering of Guaratinguetá, Institute of Bioenergy Research (IPBEN-UNESP)—Associated Laboratory of Guaratinguetá, Laboratory of Optimization of Energy Systems (LOSE), São Paulo State University UNESP, Guaratinguetá 12516-410, Brazil; victor.campos@unesp.br (V.A.F.d.C.); joseluz@feg.unesp.br (J.L.S.)

<sup>5</sup> VALORIZA—Research Center for Endogenous Resource Valorization, Polytechnic Institute of Portalegre, 7300-555 Portalegre, Portugal; pbrito@ippportalegre.pt

\* Correspondence: rpanizio@ippportalegre.pt (R.M.-P.); mhorzaez@ujaen.es (M.J.H.-O.); Tel.: +34-610-389-020 (M.J.H.-O.)

Received: 7 October 2020; Accepted: 17 November 2020; Published: 20 November 2020



**Abstract:** The recovery of noble metals from electrical wires and cables results in waste materials such as polyvinyl chloride (PVC) and polyethylene (PE), that is, waste insulation electrical cables (WIEC), which have been processed by gasification for energy recovery. This study focused on the effect of blending the ratio of WIEC on the gasification feedstock composition and the lower heating value (LHV) of produced syngas, through controlled tests and tests under different loads on the generator. The controlled gasification experiments were carried out at blending ratios between pine biomass and WIEC of 90:10, 80:20, and 70:30 and with pine biomass only (100%). For the loads gasification, the experiments were carried out at a blending ratio of 80:20. The controlled experimental results presented that the highest hydrogen content, approximated 17.7 vol.%, was observed at a blending ratio of 70:30 between pine biomass and WIEC and the highest LHV of syngas was observed at a blending ratio of 90:10, with 5.7 MJ/Nm<sup>3</sup>. For the load gasification experiments, the results showed that the highest hydrogen content was obtained with a load of 15 kW in the generator, approximately 18.48 vol.% of hydrogen content, and the highest LHV of synthesis gas was observed during the 5 kW test, with 5.22 MJ/Nm<sup>3</sup>. Overall, the new processing of waste insulation electrical cables using a downdraft gasification reactor demonstrates great promise for high quality syngas production.

**Keywords:** gasification; WEEE; waste insulation electrical cables; energy recovery; biofuel

## 1. Introduction

For the development of countries to take place, investments related to the form of production and generation of electricity are necessary. On the basis of current demands, and especially the relationship between man and nature, investments must be made to generate clean and renewable energy. Therefore, an economic development is needed in accordance with the social aspect, aiming at the preservation of the environment, and thus generating sustainable development [1].

Renewable resources have gained attention around the world as a source of energy. The use of biomass to generate electrical energy has been used as a renewable energy source to reduce the environmental impacts produced by excessive energy consumption. Similar to other energy resources, the use of biomass has limitations in terms of use and applicability, however, it can compete directly with fossil fuels, and also with other energy sources, such as wind, solar and wave energy [2]. In this sense, biomass can be used as energy and chemicals, and may partially replace energy sources such as fossil fuels [3]. According to the Renewable Energy Policy Network for the 21st Century (REN21), the use of biomass as a source of heat has even surpassed its use in electricity or transportation [4].

Petroleum is currently considered to be the main source of energy; however, research is underway to replace a significant percentage of fossil fuels with the use of renewable sources, and thus follow the global search to rethink the sources of energy generation in order to achieve development and preservation of the environment [5].

One way is by the conversion of biomass through different processes, namely, biochemical, chemical, and thermochemical. There are several types of biomass conversion technologies for small- and large-scale applications, including processes such as gasification, heat and electricity production (cogeneration), energy recovery from solid urban waste, biogas from landfills, and biofuels for application in the transport sector.

In the thermochemical conversion process, biomass is converted into gases, liquid fuels, or coal [6]. Gasification is a thermochemical process that transforms carbon-rich materials, such as biomass, into gaseous fuels, and therefore includes adding sub-stoichiometric levels of an oxidant agent for partial oxidation of these carbon-rich materials (char and the high-molecular-weight volatiles) [7]. For the conversion to occur, a medium is necessary, and gas has usually been used, however, recent studies have used supercritical water as a medium for the gasification process, and this process has resulted in higher Lower Heating Values (LHVs) of gas produced than those obtained by air gasification. However, air gasification is the most extensively studied and applied process because the gasification agent is inexpensive, the reaction process is easy, and the reactor structure is simple. Supercritical water gasification should be better studied and developed due to the fact that reactor plugging is a critical problem when feedstocks with high biomass content are gasified, as well as other problems [6,8]. Gasification produces a synthetic gas that contains  $H_2$ ,  $CO$ ,  $CO_2$ ,  $CH_4$ , and light hydrocarbons, when under restricted oxygen conditions [9].

The thermochemical conversion process of thermal gasification involves several reactions, starting with devolatilization and the formation of char and continuing until more complex reactions such as heterogeneous and homogeneous reactions that involve the formed compounds and the gasifying medium [10].

Although there are several studies on thermochemical recovery technologies for different wastes, research based on waste electrical and electronic equipment (WEEE) is still in its infancy, with the research topics mainly focused on recycling [9,10], material recovery [11–14], environmental analysis [15], and waste characterization [16]. Few studies have focused on energy recovery by thermochemical methods, especially pyrolysis [16,17] carbonization [18–20], and gasification [21].

WEEE contains valuable metals such as copper and aluminum, which is why WEEE attracts attention for recycling [22]. Another important resource present in WEEE is plastic that occupies about 30% of its total weight. Currently, the majority of WEEE that is produced is sent to landfill or incineration without energy recovery, with a small percentage being valorized for other purposes [23]. Thus, plastic gasification means energy recovery that prevents waste from being landfilled [22,23]. At the same time, co-gasification of different materials and synergies can improve the calorific value of the produced gas [24–26].

Electrical and electronic equipment (EEE) includes a wide range of products. Directive 2012/19/EU has defined EEE as equipment that requires electric current or also involves electromagnetic fields in order to function. This classification includes equipment ranging from small appliances to information technology equipment [27].

This article studied the energy recovery of the waste insulation electrical cables (WIEC). A company located in Portugal reuses the noble metals inside the cables and the other components are sent to landfill. These coatings are composed of different plastics (polyethylene, polypropylene, polyethylene terephthalate and polystyrene), also containing in its composition quantities of metals and traces of brominated compounds. There is a large amount of plastic waste that can produce significant amounts of energy.

## 2. Materials and Methods

Generally, cables consist of a metallic interior (copper or aluminum), a semiconductor layer, and an insulating coating composed of polyvinyl chloride (PVC) or polyethylene (PE) thermoplastic material. Aiming at harnessing the noble metals inside the wires, the wiring is recycled, and the material left over from this recycling is a mixture of PVC and PE and noble metals in small quantities. Polymeric residues may be a suitable co-reagent, together with lignocellulosic biomass for thermochemical processes, namely, co-pyrolysis and co-gasification, since the vast majority of polymeric residues, such as polyethylene (PE), polystyrene (PS), polypropylene (PP), and polyethylene glycol terephthalate (PET) are rich in hydrogen and poor in oxygen. Pending an energy recovery solution, polymeric waste is disposed of in landfills, causing serious environmental problems. For this reason, co-gasification of lignocellulosic biomass and polymeric residues can be a promising method to alleviate environmental pollution and provide renewable energy.

For the tests, pine forest biomass (PFB) and waste insulation for electrical cables (WIEC) were used in different blending ratios PFB/WIEC. The gasification experiments were carried out in a gasifier comprised of a downdraft reactor, a 3.0 L 4-cylinder internal combustion engine coupled with a 20 kW electric power generator, and an electronic control unit. Several controlled gasification tests were carried out, that is, without the engine and the generator running, to identify the effect of the blending ratio. Four tests were carried out with pine forest biomass and cables in different blending ratios, i.e., 100:0, 90:10, 80:20, and 70:30.

Three co-gasification tests were carried out with loads of 5, 10, and 15 kW, with the gasifier generator assuming the effect of temperature, equivalence ratio, synthesis gas quality, and amounts of chars and tar production for the feedstock blending ratio of 80:20.

### 2.1. Analyses of Fuels

#### 2.1.1. Ultimate Analysis

The elements of interest included carbon (C), hydrogen (H), nitrogen (N), sulphur (S), and oxygen (O). The C, H, N, S, and O quantities were determined using a Thermo Fisher Scientific Flash 2000 CHNS-O analyzer.

#### 2.1.2. Thermogravimetric Analysis

Thermogravimetric analysis was used to determine the moisture content, volatile matter, and fixed carbon combined with ash. The tests were performed in triplicate with sample weights between 7 and 10 mg. A PerkinElmer, STA 6000 thermogravimetric analyzer was used, using a nitrogen flow of 20 mL/min for an inert atmosphere and a temperature growth rate of 20 °C/min. The content of each type of matter was determined from the thermogravimetric profile (variation of the sample mass versus temperature), considering the inflection points of the mass derivative as a function of time.

#### 2.1.3. Higher Heating Value Analysis

The higher heating values (HHVs) of the fuels were calculated on the IKA C 2000 calorimetry equipment, through the complete combustion of samples in an adiabatic environment. For the determination of the HHV, a sample with  $0.5 \pm 0.1$  g of each fuel was placed in the calorimeter and its total combustion was carried out. The experiments were executed in triplicate.

### 2.1.4. X-Ray Fluorescence (XRF)

The amount of chlorine present in WIEC was monitored by X-ray fluorescence analysis, in order to verify the viability of the process. The analysis was determined by X-ray fluorescence analysis using a Thermo Scientific Niton XL 3T GoldD+ analyzer.

### 2.2. Gasification Test

The gasification tests were performed on an AllPowerLabs PP20 Power Pallets - a gasifier with a power of 15kW, illustrated in Figure 1, a common downdraft reactor that is combined with an electric power generator and an electronic control unit. The equipment consists of a storage silo, where the biomass is simultaneously dried by recirculating the hot gases produced in the reactor. Fuel is supplied from the top as the air moves downward, being preheated through contact with the reactor's walls. It should be noted that the gasifier admits grinded raw material, with dimensions between 1 to 4 cm. Pine biomass had these characteristics and was grinded before the process. Insulation residues for electrical cables (WIEC) have dimensions between 0.2 and 1 cm, that is, they have been reduced during the metal removal process.

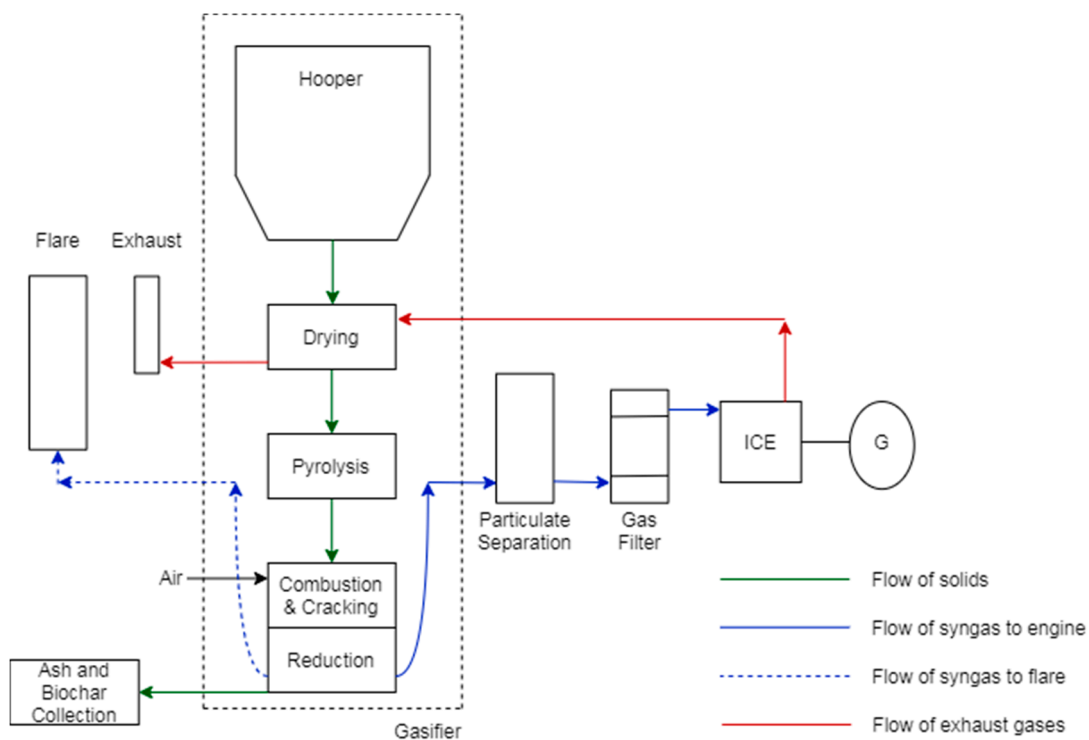


Figure 1. Gasifier schematics adapted from [28].

At the bottom of the reactor there is a char collection system, using an endless screw, which pushes the unconverted material into an accessory tank. The synthesis gas leaves the reactor at a temperature between 450 to 550 °C. Downstream of the reactor there is a cyclone filter, which removes the finer particles that follow with the synthesis gas produced. Then the synthesis gas is taken to a heat exchanger, whose function is to reduce the temperature of the synthesis gas to below 100 °C and, at the same time, to heat the biomass found in the hopper. Subsequently, the synthesis gas is cleaned through a filter composed of biomasses of various granulometries. In this filter, there are the retention of tars, which are condensed there. The clean synthesis gas, with a temperature of 50 to 70 °C, can be collected for analysis or injected directly into the engine. Condensed matter is collected at the bottom of the biomass filter

The Otto cycle internal combustion engine (ICE) burns the gas providing kinetic energy for the generator. In order to start the engine according to the manufacturer's instructions, the temperature in the reactor's lower part (reduction zone) must be at least 400 °C.

The tests were carried out in co-gasification with pine, biomass material that presents some good characteristics for gasification and produces low ash/char content. For the beginning of the experiment it was used 100% pine forest residue, which was the standard biomass for the tests.

During each test, lasting 180 minutes, some parameters were controlled, namely the values of temperature (the temperature sensors are welded outside the reactor, next to the air inlet) and pressure in the upper and lower parts of the reactor (oxidation and reduction zones, respectively), pressure in the biomass particle filter, inlet airflow rate and lastly the amount of biomass consumed during the test. The gas samples were collected from the biomass particle filter into suitable bags with the aid of a vacuum pump in the minutes 60, 120 and 160, for all the experiments. The chars were trapped in the bottom of the reactor and in the cyclone filter, which was downstream of the reactor. The condensates were collected at the bottom of the biomass particulate filter.

### 2.3. Gasification Products Analysis

#### 2.3.1. Synthesis Gas

Analysis of the synthesis gases was performed by gas chromatography. Each bag containing the synthesis gas was analyzed using a peristaltic pump to affect the injection of the samples, where the components were separated through a set of specific columns using helium and nitrogen as carrier gases.

The gases were analyzed on a Varian 450-GC Gas Chromatograph with a Thermal Conductivity Detector (TCD) (used for identification and quantification of gaseous constituents CO, CO<sub>2</sub>, H<sub>2</sub>, CH<sub>4</sub>, and light hydrocarbons present).

#### 2.3.2. Tars

Thermal gasification converts fuel into syngas with chars and tar as byproducts formed during the process which restricts practical applications. These byproducts are also harmful to the environment and human health, therefore, it is essential to reduce their production [29]. To evaluate the quantity of tar production during the tests, as previously mentioned, the tars condense and are retained in the bottom biomass filter well, as in the piping end where they are condensed due to temperatures below 300 °C (last stage before the flare). At the end of the process, it was possible to remove and measure the volume produced.

#### 2.3.3. Chars

Similar to tars, the solid fraction produced during gasification was also determined. The chars were collected in the cyclone filter and in the ash collector.

#### 2.3.4. Theoretical Parameters

To estimate the volumetric air mass entering the reactor, an appropriate flowmeter was used, which was located at the equipment's air intake. Because the equipment did not have a flowmeter to measure the synthesis gas produced, an equation was used, in which the amount of volumetric air entering the reactor was combined with the percentage of nitrogen present in the synthesis gas [30] as follows:

$$V_{syngas} = V_{air} \left( \frac{0.781}{N_2} \right) \quad (1)$$

where  $V_{syngas}$  is the volumetric flow of syngas in Nm<sup>3</sup>/h,  $V_{air}$  is the volumetric flow of air in Nm<sup>3</sup>/h, 0.781 is the nitrogen percentage in the air, and  $N_2$  is the nitrogen percentage in the syngas.

Taking advantage of the need to calculate the volume of syngas, the equivalence ratio was calculated. The equivalence ratio is commonly used to indicate quantitatively whether a fuel oxidizer mixture is rich, lean, or stoichiometric. The equivalence ratio is defined as the actual air/fuel ratio (used in the gasification) to the stoichiometric air/fuel ratio for combustion [31] as follows:

$$ER = \frac{(A/F)}{(A/F)_{stoic}} \quad (2)$$

where  $ER$  is the equivalence ratio;  $(A/F)$  is the same mass ratio but under the experimental conditions that were adopted, and  $(A/F)_{stoic}$  is the mass ratio of air/fuel at stoichiometric conditions.

Therefore, for rich mixtures, the equivalence ratio ( $ER$ ) was  $>1$ ; for poor mixtures,  $ER < 1$ ; and for stoichiometric mixtures,  $ER = 1$ .

Gasifier efficiency, total efficiency, and engine efficiency are calculated as follows:

$$\eta_{gas} = \frac{(V_{syngas} \cdot LHV_{syngas})}{(m_{bio} \cdot LHV_{bio})} \quad (3)$$

$$\eta_{tot} = \frac{E_{el} \cdot 3.6}{(m_{bio} \cdot LHV_{bio})} \quad (4)$$

$$\eta_{eng} = \frac{(\eta_{tot} \cdot \eta_{gen})}{\eta_{gas}} \quad (5)$$

where  $\eta_{gas}$  is the gasifier efficiency,  $LHV_{syngas}$  is the syngas lower heating value,  $m_{bio}$  is the fuel mass used during the test,  $\eta_{tot}$  is the total efficiency,  $LHV_{bio}$  is the fuel lower heating value,  $E_{el}$  (kWh) is the electrical energy generated during the test,  $\eta_{eng}$  is the engine efficiency, and  $\eta_{gen}$  is the generator efficiency. Once the electrical energy generated is determined, the mass of biomass necessary to generate this energy in kg/kWh can be estimated.

### 3. Results and Discussions

#### 3.1. Biomass Characterization

Table 1 exposes the values of the proximate analysis (moisture, volatile matter and fixed carbon), ultimate analysis (C, H, N, and S), and high heating value.

**Table 1.** Fuel analysis.

Analysis	Parameters	Units	Fuels	
			Pine	WIEC
Proximate	Moisture	%	7.43	0.79
	Volatile matter	%	53.61	68.4
	Fixed carbon	%	36.36	30.51
	Ashes	%	2.6	2.3
Ultimate	Nitrogen	%	0.6	0.2
	Carbon	%	49.7	52.3
	Hydrogen	%	7.5	2.5
	Sulphur	%	0	0
	Oxygen	%	39.8	42.7
	HHV	MJ/kg	18.4	22.7
	XRF	%	0.04	0.55

### 3.2. Heating Values

From the chemical elements present in biomass (C, H, N, S, and O), carbon is the main element, which has a high calorific value of 34 MJ/kg and presents a percentage fraction in the order of 40% to 75% in fuel composition solids and about 83% to 85% in oil fuels [32]. At the same time, hydrogen has a higher calorific value of 120 MJ/kg, however, the percentage fraction in the composition of solid fuels is very small, in the order of 2% to 8%, and slightly higher in liquid fuels (10% to 12%).

The HHV obtained, in the case of the WIEC of 22.7 MJ/kg, is slightly higher than pine. The amount of carbon present in WIEC is responsible for the high energy value.

For the pine biomass, the HHV had similar values to other forestall biomass. The difference between the two fuels resides in less hydrogen in the WIEC composition, and also the fact that the pines were in chips which caused them to present more humidity (more hydrogen content), and hence lower calorific value.

### 3.3. Proximate Analyses

Table 1 presents the results from proximate and ultimate analyses and high heat values. The proximate analysis demonstrates that both fuels have quite different attributes, regarding its characteristics.

The moisture content varied between 7.43% for pine and 0.8% for WIEC, that is, both fuels are suitable for thermochemical applications. It is considered that in thermochemical processes, such as gasification and combustion, the moisture parameter should not exceed 30%. However, the thermal gasification process allows for relatively higher moisture than the combustion process, since most gasifiers use part of the thermal energy generated in the reactor, to predry the fuel before it enters the reactor.

The high content of volatile matter that the WIEC fuel presents (68.4%), indicates that a relatively lower amount of thermal energy is necessary to initiate thermochemical reactions, that is, this fuel is considered to be suitable for the thermal gasification process at lower temperatures as compared with fuels that have a higher amount of fixed carbon. However, a higher amount of VM increases the HHV but also causes a higher probability of tar formation. This observation can be seen in Table 1.

Regarding the biomass pine fuel, the amount of volatile matter (53.61%) is lower than WIEC fuel. As previously mentioned, fuels with moderate amounts of VM are advantageous for the thermal gasification process since the risks of tar production are reduced, avoiding bridging and problems related to bad combustion in internal combustion engines, which are often used in this type of process to generate energy.

The fixed carbon contents of WIEC and pine are relatively close, with 30.51% and 36.36%, respectively. When the loss of volatile content is greater in the fuel, the fixed carbon residue diminishes. The high content of fixed carbon benefits the thermochemical processes since the energy density of the fuel increases with an increase in this parameter, which translates into a high energy efficiency in the gasifier. A very relevant aspect is that the fixed carbon in a gasification reactor is responsible for increasing the temperature, and is also a determinant for the thermal cracking of the tar produced during the gasification process [33].

The ash contents of the two fuels are very similar, about 3% for pine and 2% for WIEC. The ash content for both fuels is considered to be suitable for thermochemical processes, since fuels with an ash content above 7% tend to form slag in thermochemical processes, mainly at high temperatures (around 1000 °C). This aspect can be problematic for the system, since it can lead to excessive formation of tar, blockages, and malfunction of the reactor. The high ash content of the fuel is also responsible for the reduction in the HHV. The thermal gasification process by means of a downdraft reactor is the most appropriate when a fuel has a high ash content, because of the constant removal of unconverted material and ashes at the bottom of the reactor, which prevents the referred problems.

### 3.4. Ultimate Analysis

The carbon content in biomass varieties, usually ranging from 44.1% to 75.5% [34]. For the case of pine, the value was 48.7%, which corresponded to typical forestall biomass. For WIEC, the value was 52.3%. The chemical element C is the principal element in all combustible material and is responsible for the HHV of all fuels. Alternatively, hydrogen content in the pine was 7.5% and for WIEC it was 2.5%. Hydrogen presents a high HHV, but the percentage of this chemical element in fuels is very low and is related to the moisture of the biomass. In the case of WIEC, it is near null, because this material was dried and does not have the characteristics of forestall biomass to retain water.

The nitrogen content in pine was 0.6% and in the WIEC it was 0.2%. The presence of nitrogen in a fuel can be harmful in a thermochemical process, namely combustion, due to the formation of NO<sub>x</sub>. Usually, lignocellulosic biomasses tend to not exceed more than 1% content of this element [35]. Therefore, a low nitrogen content in a fuel means that NO<sub>x</sub> formation during thermochemical conversion is minimal. Another important aspect, when NO<sub>x</sub> formation is addressed in the thermal gasification process, oxygen enters the reactor in an amount lower than stoichiometry, and therefore there is more formation of CO and CO<sub>2</sub> than NO<sub>x</sub>, in addition, the low gasification temperatures (below 900 °C) prevent the formation of thermal NO<sub>x</sub>.

Regarding sulfur, pine biomass did not show any percentage of this element. Similar to the presence of nitrogen in the fuel, the absence of sulfur is also beneficial in its use in energy conversion, since it decreases the formation of SO<sub>2</sub>.

The oxygen content in the pine was 42.2% (dry bases) and 45% (dry bases) for WIEC. This element has a significant influence regarding the fuel HHV, hence it is important, sometimes, to pretreat the fuel and deoxidize it in order to increase the HHV.

## 4. Results

### 4.1. Controlled Gasification Results

Table 2 presents the results obtained in the co-gasification, the PFB/WIEC in the blending ratio (100:0, 90:10, 80:20 and 70:30) experiments, namely, values of production, composition, lower heating value (LHV) of gases, and chars and tars as a function of co-gasification mixture.

### 4.2. Controlled Gasification Syngas Composition

In the gasification tests, the samples were taken at 60, 120, and 180 min, as a criterion and in order to be able to observe the evolution of the synthesis gas produced, until the process stabilized. It should be noted that the temperature of the first sample (60 min) is constantly low, it is still a transitory phase of the process, when the temperature is rising. In the second sample, the temperature of the process is still rising, however, the inertia of the equipment is much lower, and the stabilization of the process is more noticeable, not extinguishing a large amount of oxidizing agent, as in the first sample. The third sample is considered to be the stabilization of the process, where the temperature variation is zero or nearly zero. As previously mentioned, the temperature sensors are welded on the outer wall of the reactor, for this reason, the oxidation and reduction temperatures may appear to be lower as compared with a normal gasification process.

Table 2. Gasification results.

Parameters	Units	100:0			90:10			80:20			70:30		
		Sample 1	Sample 2	Sample 3	Sample 1	Sample 2	Sample 3	Sample 1	Sample 2	Sample 3	Sample 1	Sample 2	Sample 3
CO <sub>2</sub>	%	12.78	9.16	8.52	11.52	10.51	10.82	9.95	9.80	9.1	10.01	10.71	9.84
C <sub>2</sub> H <sub>4</sub>	%	0.82	0.57	0.17	0.84	0.68	0.63	0.74	0.21	0.22	0.59	0.35	0.26
C <sub>2</sub> H <sub>6</sub>	%	0.21	0.15	0.04	0.18	0.15	0.14	0.02	0.01	0.02	0.02	0.01	0.01
C <sub>2</sub> H <sub>2</sub>	%	0.04	0.02	0.04	0.03	0.08	0.25	0.01	0.01	0.01	0.01	0.00	0.00
H <sub>2</sub> S	%	0.00	0.00	0.00	0.00	0.00	0.00	0.00	0.00	0.00	0.00	0.00	0.00
N <sub>2</sub>	%	57.09	56.58	52.27	58.84	53.60	50.33	57.73	55.13	51.60	56.31	51.09	49.66
CH <sub>4</sub>	%	3.21	2.24	2.04	3.09	2.70	2.62	1.47	1.71	1.58	2.05	1.46	1.42
CO	%	15.11	18.77	19.91	14.90	19.24	19.44	18.04	20.11	20.50	19.02	20.85	20.47
H <sub>2</sub>	%	10.73	12.91	15.42	11.30	14.58	15.75	12.02	12.95	16.79	12.26	14.52	17.68
LHV	MJ/m <sup>3</sup>	4.85	5.01	5.06	4.83	5.51	5.70	4.57	4.70	5.12	4.84	4.95	5.18
Trst	°C	507.00	603.00	720.00	594.00	615.00	708.00	614.00	699.00	758.00	627.00	718.00	789.00
Tred	°C	289.00	484.00	515.00	371.00	499.00	547.00	274.00	476.00	526.00	395.00	485.00	532.00
Pcomb	KPa	−19.00	−16.00	−12.00	−19.00	−17.00	−10.00	−19.00	−12.00	−12.00	−17.00	−13.00	−12.00
PReact	KPa	−46.00	−23.00	−22.00	−22.00	−22.00	−25.00	−26.00	−27.00	−24.00	−25.00	−23.00	−28.00
Pfilt	KPa	−60.00	−46.00	−40.00	−45.00	−39.00	−32.00	−49.00	−45.00	−45.00	−48.00	−45.00	−52.00
Vair	m <sup>3</sup> /h	11.51	10.94	10.03	12.42	10.45	8.89	11.48	10.46	9.26	11.00	9.88	9.00
Tair	°C	12.70	14.90	15.80	15.70	19.30	19.60	11.30	14.40	15.60	12.40	15.80	18.20
Vtars	g/Nm <sup>3</sup> syngas		8.54			9.88			10.97			12.31	
Vchars	kg/h		0.16			0.17			0.16			0.19	
ER	-	0.28	0.27	0.24	0.30	0.25	0.16	0.26	0.24	0.20	0.25	0.22	0.19
Cold gas efficiency	%	80.05	78.54	79.67	65.94	69.17	65.66	54.35	53.74	54.85	55.47	55.98	54.44
Vsyngás	m <sup>3</sup> /h	15.78	15.00	15.07	16.44	15.12	13.89	15.46	14.86	13.91	15.34	15.13	14.06
Sample collection	min	60	120	160	60	120	160	60	120	160	60	120	160
Fuel flow	kg/h		5.20			6.40			6.90			7.10	
Experiment time	min		180.00			180.00			180.00			180.00	

Figure 2 illustrates the composition of syngas produced for each experiment. In fact, the WIEC content is responsible for the difference in temperature distribution in the reactor throughout the tests, which is reflected in the syngas composition. It is possible to observe that the temperature increases with an increase in the percentage of WIEC, due to large amounts of volatiles. The volatiles are released as the temperature increases; for lignocellulosic biomass, the devolatilization occurs at higher temperatures, around 500 °C. WIEC have higher amounts of volatiles that require lower temperatures to devolatilize, which increases temperatures during the thermochemical process. A positive impact is observed with an increase in WIEC on the behavior of the temperature and in the concentrations of H<sub>2</sub> and CO, while other studies have also reported a decrease in CO<sub>2</sub> concentration and an increase in H<sub>2</sub> concentration with higher proportions of polymeric residues in mixtures with pine [36]. The test performed with a mixture of 30% WIEC presented higher temperatures in the combustion and reduction zones and concentrations of H<sub>2</sub> of 17.7% and CO of 20.5%, originating a syngas with a HHV of 5.18 MJ/m<sup>3</sup>. Another study by Ahmed et al. determined an alternative influence with a mixture of lignocellulosic and plastic fuels and concluded that the chars derived from the lignocellulosic fuel absorbed the volatiles of the polymeric fuel, and therefore promoted the cracking of these hydrocarbons. The polymeric radicals acted as H contributors that balanced the radicals formed by the lignocellulosic fuel [37]. These mixtures, contrary to expectations, produced a reduced number of light hydrocarbons, and increased the concentration of CO and H<sub>2</sub>. The quality of the syngas is indicative of improved catalytic reform. These results may be related to the formation of lignocellulosic fuel chars.

With an increase in the percentage of WIEC, and the consequent increase in the reactor temperature, it is possible to observe that the Boudouard reaction ( $C + CO_2 \rightleftharpoons 2CO$ ) of CO is favored and, additionally, light hydrocarbons suffer cracking reactions at high temperatures favoring H<sub>2</sub> formation.



Figure 2. Syngas composition.

#### 4.3. Controlled Gasification Theoretical Parameters

Regarding theoretical parameters, the cold gas efficiency (CGE) is a function of LHV, syngas, and fuel flow. The LHV is influenced by the ER, i.e., when ER decreases, the LHV tends to increase, and gasification efficiency also increases. In order to maintain the ideal operating conditions of a commercial gasifier, it is normally operated with an equivalence ratio of 0.25 [38]. Air intakes in the reduction zone increase the rate of the devolatilization reaction due to pyrolysis and heterogeneous oxidative reactions.

However, when the ER increases, the concentration of CO<sub>2</sub> present in syngas tends to increase, while the concentrations of CO and H<sub>2</sub> decrease. The gasification temperature is mainly responsible for the directional change in the balance of gasification reactions. For example, endothermic reactions tended to change directly with increasing temperature or indirectly with decreasing temperature. Therefore, when there is an increase in ER, the conversion of carbon into CO and H<sub>2</sub> is highly reduced, favoring other products, mainly CO<sub>2</sub> [39]. Although the rate of gas production increases and the CGE increases, the calorific value of syngas decreases, and the efficiency of gasification also decreases (Figure 3), with steam responsible for contributing to the water-gas reaction and the greater the value, the lower the conversion to synthesis gas [40]. For comparison of the different operating temperatures, the yield of synthesis gas decreased with an increase in temperature, indicating that the high temperature may not have been as beneficial for the production volume as for the quality of the syngas. An increase in ER leads to a poorer syngas composition, because of the N<sub>2</sub> dilution effect, and also because the H<sub>2</sub> and CO contents decrease. With high ER, more oxidizing agent enters in the process, therefore, higher CO<sub>2</sub> content is observed, and it can be concluded that combustion reactions are dominant over gasification reactions.

For the study carried out, the highest CGE was 80.1, with an ER of 0.28 to 100% pine chip, and the minimum was obtained in the 80:20 test, i.e., a CGE of 53.7 and a 0.24 ER. Regarding the effect of ER on CGE, it is not relevant since the concentration of CO, H<sub>2</sub>, and CH<sub>4</sub> contributes to an increase in the HHV of syngas and ER close to 0.2 [41]. In addition to this point, since the yield of the products above decreased and the consumption of biomass increased as WIEC was added, CGE follows a downward trend.



Figure 3. Syngas Lower Heating Value (LHV).

#### 4.4. Controlled Gasification: Chars and Tars

There is a close relationship between both fractions, tar and char. As shown in Table 1, there is a decrease in chars (relation to the fuel consumed) as the amount of WIEC increases, and also the concentration of tar increases. This is due to the increase in the volatile component of WIEC and also to thermal cracking reactions between chars and tars. An example of what was mentioned is when the air reacts with the carbons in the reduction zone. When this process occurs, it generates an activation of the carbon with the O that is present in the air and which is at temperatures above 350 °C [42].

When there is a relatively low ER, it appears that the air present in the reduction zone is very low, thus, generating the non-activation of the coal, even if the temperature in this region is equal to or higher than the temperature required for activation [43]. The structure and distribution of the pores present in the chars were altered due to their extension. The surface area is reduced, and therefore the tar can be captured more easily [44]. When the temperature of the air reached the reduction zone above 350 °C, it activated the charcoal, producing the most extensive pores and reducing the surface area. The diameter of the carbonized particles became smaller as a result of degradation and erosion. When air passed through the pores, diffusion occurred, causing damage to the micro- and mesopores, forming walls between them. This increase in pores resulted in a reduction in the surface area of the coal. As an advantage of the increase in pore size, one can consider the greater rate of capturing components such as tar, due to the greater facility of gas passing through the pores [45].

In the tests carried out, it was possible to observe a lower concentration of tar when the fuel used was pine biomass, followed by the test with incorporation of 10% WIEC, due to the greater amount of air admitted in the reduction zone. Because of this, there was a balance for both the temperature and the retention time between the reduction zone, with the reforming tar and the oxidation zone cracking tar. When the amount of air in the reduction zone remains constant, the amount of tar tends to increase. This phenomenon occurs because the flow rate is constant, causing a layer of ash to cover the surface of the coal, reducing absorption.

#### 4.5. Load Gasification Experiments

Table 3 presents the results obtained in the co-gasification (80:20) experiments, namely, values of production, composition, LHV of gases and chars and tars, under electrical loads of 5, 10, and 16 kW.

**Table 3.** Gasification of pine forest biomass (PFB) and waste insulation electrical cables (WIEC) in blending ratio 80:20, with electrical loads of 5, 10, and 15 kW.

Parameters	Units	5 kW			10 kW			15 kW		
		Sample 1	Sample 2	Sample 3	Sample 1	Sample 2	Sample 3	Sample 1	Sample 2	Sample 3
CO <sub>2</sub>	%	12.40	12.50	11.80	13.21	12.75	12.81	13.03	13.89	12.05
C <sub>2</sub> H <sub>4</sub>	%	0.20	0.08	0.09	0.10	0.07	0.03	0.05	0.05	0.06
C <sub>2</sub> H <sub>6</sub>	%	0.02	0.01	0.01	0.05	0.07	0.05	0.02	0.01	0.02
C <sub>2</sub> H <sub>2</sub>	%	0.02	0.02	0.01	0.01	0.08	0.04	0.01	0.02	0.01
H <sub>2</sub> S	%	0.00	0.00	0.00	0.00	0.00	0.00	0.00	0.00	0.00
N <sub>2</sub>	%	52.12	51.78	51.03	49.69	52.07	50.10	53.98	52.82	52.02
CH <sub>4</sub>	%	2.58	2.35	2.41	2.37	2.04	2.38	1.87	1.04	1.01
CO	%	17.35	18.96	18.89	18.35	18.57	19.02	16.84	17.86	19.07
H <sub>2</sub>	%	16.42	16.04	17.62	16.21	16.08	16.84	16.58	16.32	18.48
LHV	MJ/m <sup>3</sup>	5.03	5.03	5.22	5.01	4.94	5.15	4.64	4.44	4.82
T <sub>rst</sub>	°C	883.00	889.00	895.00	879.00	885.00	888.00	913.00	947.00	958.00
T <sub>red</sub>	°C	613.00	625.00	657.00	621.00	658.00	671.00	607.00	643.00	687.00
P <sub>comb</sub>	KPa	-25.00	-22.00	-23.00	-18.00	-25.00	-26.00	-27.00	-28.00	-26.00
P <sub>React</sub>	KPa	-51.00	-46.00	-45.00	-39.00	-48.00	-53.00	-59.00	-64.00	-62.00
P <sub>filt</sub>	KPa	-67.00	-64.00	-68.00	-64.00	-72.00	-78.00	-81.00	-86.00	-84.00
V <sub>air</sub>	m <sup>3</sup> /h	11.76	11.21	11.07	18.88	20.63	19.35	34.97	33.86	33.56
T <sub>air</sub>	°C	13.10	14.80	16.20	13.20	15.30	18.90	12.70	15.70	19.20
V <sub>tars</sub>	g/Nm <sup>3</sup> <sub>syngas</sub>		4.20			7.54			8.79	
V <sub>chars</sub>	kg/h		0.28			0.34			0.47	
ER	-	0.27	0.25	0.25	0.23	0.25	0.23	0.28	0.27	0.27
Cold gas efficiency	%	80.91	77.15	80.59	71.03	73.57	74.82	74.76	70.56	77.38
V <sub>syngas</sub>	m <sup>3</sup> /h	17.66	16.84	16.95	29.49	30.98	30.22	50.58	49.89	50.40
Sample collection	min	60.00	120.00	160.00	60.00	120.00	160.00	60.00	120.00	160.00
Q <sub>biomass</sub>	kg/h		5.70			10.8			16.3	
Experiment time	min		180.00			180.00			180.00	

The 80:20 mixing ratio was considered to be the most interesting for the use and energetic valuation of WIEC, despite having a calorific value of syngas that was 10% lower than that obtained in the 90:10 mixing ratio. Greater incorporation of waste allows better use of polymeric waste for energy recovery. Regarding the 70:30 mixture not being considered, this is due to the fact that there is a drastic increase

in temperatures inside the reactor during the gasification tests, since the operation with load tends to increase the temperature a lot and results in problems with agglomeration materials.

#### 4.6. Load Gasification Analysis

Syngas composition depends strongly on gasification temperature, since the mixture for all tests is the same [46]. When working with a load (engine controlling the operation) the suction of the engine is greater than the vacuum pumps (controlled tests by vacuum pumps), leading to an increase in temperature inside the reactor, an increase in the air intake, and higher consumption of biomass.

The volumetric fractions of the combustible gases CO, H<sub>2</sub>, and CH<sub>4</sub> present in syngas in the co-gasification tests at different loads are shown in Figure 4. Similar to the controlled tests, samples were taken at 60, 120, and 160 min.

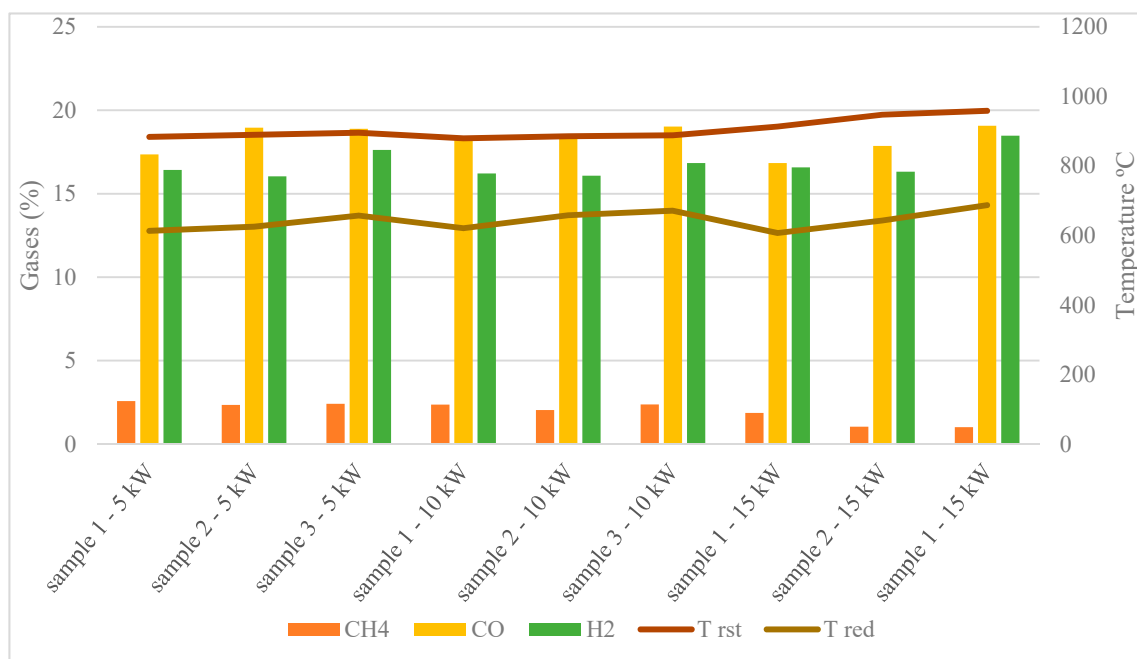


**Figure 4.** Syngas composition as function to engine loads.

The main gases found in the synthesis gas are CO, H<sub>2</sub>, and CH<sub>4</sub>, which are resulted from the reduction process occurring inside the reactor, and their concentrations may vary according to the temperature [47]. During the tests performed, the largest volume fraction is of CO followed by H<sub>2</sub>. The CO concentration reaches optimum when the amount of air in the reduction zone decreases. Under these conditions, the partial oxidation reaction of char and air in the reduction zone results in an increase in CO and temperature. This is due to the water-gas shift reaction producing more CO than H<sub>2</sub> and CH<sub>4</sub>. This tends to increase with higher temperatures, although H<sub>2</sub> production also tends to increase, as shown by the sequence of reaction rates gas water > Boudouard >> methan [6]. Thus, it makes sense that the volumetric fraction of CO is always higher than the other gases present in syngas for all tests performed and all equivalence ratios obtained. Another interesting aspect is the decrease in small hydrocarbons (C<sub>2</sub>H<sub>4</sub>, C<sub>2</sub>H<sub>6</sub>, C<sub>2</sub>H<sub>2</sub>, and CH<sub>4</sub>) as the load increases and as the temperature increases, which may be related to a growth in the reform/cracking reactions.

The water-gas shift reaction contributes more to the formation of CO and H<sub>2</sub> than the Boudouard reaction. With high temperatures in the reduction zone, it is possible to notice that the Boudouard reaction contributes to increase the conversion of CO<sub>2</sub> and CO, as can be seen in Figure 4. There is a direct relationship, i.e., when the temperature in the reduction zone increases, the concentrations of CO and H<sub>2</sub> in the syngas also increase. The maximum volumetric fraction of CO in syngas, during the different loads, was 19.07% for 15 kW, 19.02% for 10 kW, and 18.96% for 5 kW. Meanwhile, the

maximum values for H<sub>2</sub> were 17.62% for 5 kW, 16.84% for 10 kW, and 18.48% for 15 kW. As the reaction of methane occurs at a lower speed, the volume fraction of CH<sub>4</sub> is the lowest as compared with the tested loads, that is, less than 2.5%.

#### 4.7. System Efficiency for the Blending Ratio 80:20 for PFB/WIEC

Regarding the theoretical parameters, it is possible to state that when LHV increases, the ER also increases, and CGE also increases.

Larger ER are associated with oxidation reactions with a higher rate than thermal cracking reactions [48] and, eventually, an increase in CO<sub>2</sub> and N<sub>2</sub> concentrations. However, the concentrations of CO and H<sub>2</sub> in the syngas tend to decrease. If one compares the reduction in the concentration of H<sub>2</sub> with the increase in the ER, it is possible to notice that it does not increase due to the presence of polymeric as compared with the forest biomass. The presence of higher concentrations of volatile material in WIEC increases the amount of tar produced. Therefore, the cracking and tar adsorption reactions with high ER, maintain a high operating temperature which helps in increasing the H<sub>2</sub> concentration [49]. In addition, with the improvement of the ER, an evolution in the concentrations of H<sub>2</sub> and CO was noted. This was the case presented in a gasification by Toledo et al. [50], in which, while there was a reduction from 0.38 to 0.25 of the ER, it was observed that the percentage of H<sub>2</sub> and CO increased to 33% and 70%, respectively. It can be noted that ER has a variation of 0.05 between tests, where the minimum ER obtained is 0.23 and the maximum ER is 0.28 for the 10 kW and 15 kW tests, respectively. During each test, another observation was that the ER tended to decrease, except for the 10 kW test, where a lower LHV of the synthesis gas led to the engine needing more fuel, and consequently more oxidizing agent entering the reactor. The studies explained the effects of ER on the gasification of polymeric residues, with air as an oxidizing agent [51]. The results showed that the lowest heating value decreased from 13.42 to 7.05 MJ/Nm<sup>3</sup> when the ER was increased from 0.21 to 0.41. A similar result was also presented by Xiao et al. [52], with a higher heating value reducing from 11.3 to 5.17 MJ/Nm<sup>3</sup> when the ER was increased from 0.2 to 0.45. In Table 3, the results of some experiments, for lowest or equal temperatures, showed that for a higher ER, the H<sub>2</sub> content was higher, due to the fact that a lower temperature in the oxidation zone favored a greater capitalization of light hydrocarbons, which when entering in the reduction zone, underwent secondary cracking, producing shorter chain hydrocarbons and other products of the gas phase, such as H<sub>2</sub>. Although an increase in ER reduces the evolution of H<sub>2</sub> and CO, the high temperatures in the bed means that there is an improvement in cracking of the alkali, consequently improving the reaction of coal formation through the water-gas shift and Boudouard reactions [52]. This fact is quite visible when compared with the results of controlled tests with vacuum pumps and tests performed with the engine, where tar production was much lower.

To carry out the efficiency experiments, three electric loads were used in the generator, 5, 10, and 15 kW, with a duration of three hours for each experiment. All energy balances were considered, as shown in Table 4.

**Table 4.** System efficiency.

Parameters	5 kW			10 kW			15 kW		
	Sample 1	Sample 2	Sample 3	Sample 1	Sample 2	Sample 3	Sample 1	Sample 2	Sample 3
$\eta_{gas}$	80.91	77.15	80.59	71.03	73.57	74.82	74.76	70.56	77.38
$E_{el}$ (kW)	5	5	5	10	10	10	15	15	15
$\eta_{tot}$	0.16	0.16	0.16	0.17	0.17	0.17	0.17	0.17	0.17
$\eta_{gen}$	0.8	0.8	0.8	0.8	0.8	0.8	0.8	0.8	0.8
$\eta_{eng}$	0.16	0.17	0.16	0.19	0.18	0.18	0.18	0.19	0.18

The results in Table 4 show that the efficiency of the engine remained practically the same, regardless of the electrical load that was used, remaining between 16% and 19% throughout the tests.

However, the 10 and 15 kW loads produced the best results. This indicates that syngas is not able to make the engine run at full load, which agrees with the relevant findings by Raman and Ram [53]. Regarding the efficiency of gasifier, it is inversely proportional to the efficiency of the engine, this fact is related to the increase in the flow of fuel that enters the gasifier, decreasing the efficiency of syngas. In the case of 5 kW to 15 kW, there was an increase of about 186% in fuel consumption.

## 5. Conclusions

The main conclusions that can be drawn from the pine forest biomass tests with waste insulation electrical cable are the following:

- A mixture of PFB and WIEC can be applied in fixed bed gasifiers, since biomass was used as a bed for polymeric residues because they were inserted in the gasifier in a homogeneous way. In downdraft fixed flow beds, it was necessary for the biomass to have a size and weight that descended with gravity, the mixture of forest biomass and polymeric WIEC made the waste enter the system more easily.
- Regarding the operational problems detected during the tests, it was observed that limiting the incorporation of WIEC by a maximum of 30% was necessary for better gas quality, and thus recommended operational parameters.
- The incorporation of WIEC increased the temperature in the gasifier bed. With an increase in temperature, the biomass conversion rate increased and, consequently, the energy efficiency as a result of favoring reduction reactions. This means that the CO/CO<sub>2</sub> ratio would increase as the incorporation of WIEC increases.
- As the amount of WIEC in the blending ratio with PFB increased, we noticed that the temperature also rose. The incorporation of WIEC should not exceed 30% to prevent damage to the equipment.
- It was still possible to verify that the gas produced had a relatively stable composition, as well as LHV. It was noted that as the percentage of incorporation increased, the ER tended to suffer an increase. The highest LHV and ER obtained during the tests were 5.2 MJ/Nm<sup>3</sup> and 0.35.
- The synthesis gas obtained could be considered for use in internal combustion engines, as could be seen in the tests performed.
- In the tests using the engine, it was possible to observe that there was an increase in the gasification temperature. This factor was related to the suction of the generator.
- In tests with a load of 5 kW, the efficiency of the syngas was on average 80%. For loads of 10 and 15 kW, the efficiency was slightly lower, around 74%.
- Loads of 5, 10, and 15 kW were used for the 80:20 mixture. The efficiency of the engine increased as energy increased.
- The efficiency of the engine for the different applied loads averaged approximately 18%.

**Author Contributions:** Conceptualization, R.M.-P., M.J.H.-O., L.C.-C., and P.B.; methodology, R.M.-P., M.J.H.-O., L.C.-C., V.A.F.d.C., J.L.S., and P.B.; formal analysis, R.M.-P., L.C.-C., V.A.F.d.C., J.L.S., M.M.G., and P.B.; investigation R.M.-P., M.J.H.-O., L.C.-C., and P.B.; resources, J.L.S., M.M.G., and P.B.; data curation, R.M.-P., L.C.-C., V.A.F.d.C., and P.B.; writing—original draft preparation, R.M.-P., L.C.-C., and P.B.; writing—review and editing, R.M.-P., L.C.-C., V.A.F.d.C., and P.B.; visualization, R.M.-P., L.C.-C., V.A.F.d.C., and P.B.; supervision, J.L.S., M.M.G., P.B.; project administration, J.L.S., M.M.G., and P.B.; funding acquisition, J.L.S., M.M.G., and P.B. All authors have read and agreed to the published version of the manuscript.

**Funding:** This research received no external funding.

**Acknowledgments:** The authors are grateful for the financial support given to the project 0330\_IDERCEXA\_4\_E, Renewable Investment, Development and Energy for the Improvement of the Entrepreneurial Fabric in the regions Centro, Extremadura, and Alentejo, co-financed by the European Regional Development Fund (ERDF) through the INTERRREG. This research received no external funding; however, in this work, PhD Hermoso-Orzáez Manuel Jesús participated as a researcher in the external research at the Center Polytechnic Institute of Portalegre (Portugal) within the Ecocir International Project, Project of Cross-border Cooperation for the Introduction of the Ecological and Circular Economy through the Prevention of Improvement of Recycling, the Management and Valorization of Residues in the regions Centro, Extremadura, and Alentejo, Interreg España-Portugal. The authors are grateful to

VALORIZA, Research Center for Endogenous Resource Valorization, Polytechnic Institute of Portalegre, and also to MEtRICs, Mechanical Engineering and Resource Sustainability Center, Department of Science and Technology of Biomass, Faculty of Science and Technology, Universidade NOVA de Lisbon, Portugal. The authors, Victor Arruda and José Luz, would like to thank the Coordination for the Improvement of Higher Education Personnel (CAPES) and the Portuguese Foundation for Science and Technology (FCT) for the funding provided through the project number 88881.156267/2017-01.

**Conflicts of Interest:** The authors declare no conflict of interest.

## Abbreviations

A/F	Air/fuel
C	Carbon
C <sub>2</sub> H <sub>2</sub>	Ethyne
C <sub>2</sub> H <sub>6</sub>	Ethane
CGE	Cold gas efficiency
CH <sub>4</sub>	Methane
CO	Carbon monoxide
CO <sub>2</sub>	Carbon dioxide
EEE	Electrical and electronic equipment
$E_{el}$	Electrical energy
ER	Equivalence ratio
H <sub>2</sub>	Hydrogen
HHV	High heating value
ICE	Internal combustion engine
LHV	Low heating value
$m_{bio}$	Mass of biomass
N	Nitrogen
NO <sub>x</sub>	Nitrogen oxides
O	Oxygen
$P_{comb}$	Combustion pressure
PE	Polyethylene
PET	Polyethylene glycol terephthalate
PFB	Pine forest biomass
$P_{filt}$	Filter pressure
PP	Polypropylene
$P_{React}$	Reaction pressure
PS	Polystyrene
PVC	Polyvinyl chloride
$Q_{biomass}$	Biomass flow
S	Sulphur
$T_{air}$	Air temperature
$T_{red}$	Temperature of reduction
$T_{rst}$	Temperature of rest (oxidation temperature)
$V_{air}$	Volumetric flow of air
$V_{chars}$	Chars volume
VM	Volatile matter
$V_{syngas}$	Volumetric flow of syngas
$V_{tars}$	Tars volume
WEEE	Waste electrical and electronic equipment
WIEC	Waste insulation electrical cables
$\eta_{eng}$	Engine efficiency
$\eta_{gas}$	Gasifier efficiency
$\eta_{gen}$	Generator efficiency
$\eta_{tot}$	Total efficiency

## References

1. Veksha, A.; Giannis, A.; Yuan, G.; Tng, J.; Ping, W.; Chang, V.W.; Lisak, G.; Lim, T. Distribution and modeling of tar compounds produced during downdraft gasification of municipal solid waste. *Renew. Energy* **2018**, *136*, 1294–1303. [[CrossRef](#)]
2. McKendry, P. Energy production from biomass (part 2): Conversion technologies. *Bioresour. Technol.* **2002**, *83*, 47–54. [[CrossRef](#)]
3. Mckendry, P. Energy production from biomass (part 1): Overview of biomass. *Bioresour. Technol.* **2002**, *83*, 37–46. [[CrossRef](#)]
4. REN21. *Renewables 2019: Global Status Report*; REN21: Paris, France, 2019.
5. Prasertcharoensuk, P.; Hernandez, D.A.; Bull, S.J.; Phan, A.N. Optimisation of a throat downdraft gasifier for hydrogen production. *Biomass Bioenergy* **2018**, *116*, 216–226. [[CrossRef](#)]
6. Basu, P. *Biomass Gasification and Pyrolysis: Pratical Design and Theory*; Academic Press: Cambridge, MA, USA, 2010.
7. Murzin, D.Y.; Simakova, I.L. 7.21—Catalysis in Biomass Processing. In *Comprehensive Inorganic Chemistry II*; Elsevier: Amsterdam, The Netherlands, 2013; pp. 559–586.
8. Lu, Y.J.; Guo, L.J.; Ji, C.M.; Zhang, X.M.; Hao, X.H.; Yan, Q.H. Hydrogen production by biomass gasification in supercritical water: A parametric study. *Int. J. Hydrogen Energy* **2006**, *31*, 822–831. [[CrossRef](#)]
9. Kim, J.; Choi, Y. *Production of a Clean Hydrogen-Rich Gas by the Staged Gasification of Biomass and Plastic Waste*; Scrivener Publishing: New York, NY, USA, 2017; pp. 363–384.
10. Ponzio, A.; Kalisz, S.; Blasiak, W. Effect of operating conditions on tar and gas composition in high temperature air / steam gasification (HTAG) of plastic containing waste. *Fuel Process. Technol.* **2006**, *87*, 223–233. [[CrossRef](#)]
11. Ilankoon, I.M.S.K.; Ghorbani, Y.; Nan, M.; Herath, G.; Moyo, T. E-waste in the international context—A review of trade flows, regulations, hazards, waste management strategies and technologies for value recovery. *Waste Manag.* **2018**, *82*, 258–275. [[CrossRef](#)]
12. Xu, Y.; Zhang, L.; Yeh, C.H.; Liu, Y. Evaluating WEEE recycling innovation strategies with interacting sustainability-related criteria. *J. Clean. Prod.* **2018**, *190*, 618–629. [[CrossRef](#)]
13. Wang, R.; Xu, Z. Recycling of non-metallic fractions from waste electrical and electronic equipment (WEEE): A review. *Waste Manag.* **2014**, *34*, 1455–1469. [[CrossRef](#)]
14. Işıldar, A.; van Hullebusch, E.D.; Lenz, M.; Du Laing, G.; Marra, A.; Cesaro, A.; Panda, S.; Akcil, A.; Kucuker, M.A.; Kucht, K. Biotechnological strategies for the recovery of valuable and critical raw materials from waste electrical and electronic equipment (WEEE)—A review. *J. Hazard. Mater.* **2019**, *362*, 467–481. [[CrossRef](#)]
15. De Meester, S.; Nachtergaele, P.; Debaveye, S.; Dewulf, J.; Vos, P. Using material flow analysis and life cycle assessment in decision support: A case study on WEEE valorization in Belgium. *Resour. Conserv. Recycl.* **2019**, *142*, 1–9. [[CrossRef](#)]
16. Queralt, I.; Chimenos, J.M.; Formosa, J.; Maldonado-Alameda, A.; Pérez-Martínez, S.; Giro-Paloma, J. Characterisation and partition of valuable metals from WEEE in weathered municipal solid waste incineration bottom ash, with a view to recovering. *J. Clean. Prod.* **2019**, *218*, 61–68.
17. Luda, M.P. Pyrolysis of WEEE plastics. *Waste Electr. Electron. Equip. Handb.* **2012**, 239–263.
18. Yang, X.; Sun, L.; Xiang, J.; Hu, S.; Su, S. Pyrolysis and dehalogenation of plastics from waste electrical and electronic equipment (WEEE): A review. *Waste Manag.* **2013**, *33*, 462–473. [[CrossRef](#)]
19. Ebin, B.; Isik, M.I. Chapter 5—Pyrometallurgical Processes for the Recovery of Metals from WEEE. In *WEEE Recycling*; Elsevier: Amsterdam, The Netherlands, 2016; pp. 107–137.
20. Panizio, R.M.; Calado, L.F.C.; Alves, O.; Nobre, C.; Silveira, J.L.; Brito, P.; Gonçalves, M.M. Effect of the incorporation of biomass in the carbonization of waste electrical and electronic equipment. In *Proceedings of the Bioenergy Conference, Portalegre, Portugal, 11–13 September 2019*.
21. Gurgul, A.; Szczepaniak, W.; Zabłocka-Malicka, M. Incineration and pyrolysis vs. steam gasification of electronic waste. *Psychol. Bull.* **2018**, *624*, 1119–1124. [[CrossRef](#)]
22. Kasper, A.C.; Berselli, G.B.T.; Freitas, B.D.; Tenório, J.A.S.; Bernardes, A.M.; Veit, H.M. Printed wiring boards for mobile phones: Characterization and recycling of copper. *Waste Manag.* **2011**, *31*, 2536–2545. [[CrossRef](#)]
23. Gramatyka, P.; Nowosielski, R.; Sakiewicz, P. Recycling of waste electrical and electronic Recycling of waste electrical and electronic equipment. *J. Achiev. Mater. Manuf. Eng.* **2015**, *20*, 535–538.

24. Zhu, H.L.; Zhang, Y.S.; Materazzi, M.; Aranda, G.; Brett, D.J.L.; Shearing, P.R.; Manos, G. Co-gasification of beech-wood and polyethylene in a fluidized-bed reactor. *Fuel Process. Technol.* **2019**, *190*, 29–37. [[CrossRef](#)]
25. Carmo-Calado, L.; Hermoso-Orzáez, M.; Mota-Panizio, R.; Guilherme-Garcia, B.; Brito, P. Co-Combustion of Waste Tires and Plastic-Rubber Wastes with Biomass Technical and Environmental Analysis. *Sustainability* **2020**, *12*, 1036. [[CrossRef](#)]
26. Pinto, F.; Franco, C.; André, R.N.; Tavares, C.; Dias, M.; Gulyurtlu, I.; Cabrita, I. Effect of experimental conditions on co-gasification of coal, biomass and plastics wastes with air/steam mixtures in a fluidized bed system. *Fuel* **2003**, *82*, 1967–1976. [[CrossRef](#)]
27. Diretiva 2012/19/UE do Parlamento Europeu e do Conselho e do conselho de 4 de julho de 2012. Relativa aos resíduos de equipamentos elétricos e eletrónicos (REEE). *J. Of. da União Eur.* **2012**, L 197/38-71.
28. Ayol, A.; Tezer Yurdakos, O.; Gurgun, A. Investigation of municipal sludge gasification potential: Gasification characteristics of dried sludge in a pilot-scale downdraft fixed bed gasifier. *Int. J. Hydrogen Energy* **2019**, *44*, 17397–17410. [[CrossRef](#)]
29. Martínez-Iera, S.; Ranz, J.P. On the development of a wood gasification modelling approach with special emphasis on primary devolatilization and tar formation and destruction phenomena. *Energy* **2016**, *113*. [[CrossRef](#)]
30. Allesina, G.; Pedrazzi, S.; Allegretti, F.; Morselli, N.; Puglia, M.; Santunione, G.; Tartarini, P. Gasification of cotton crop residues for combined power and biochar production in Mozambique. *Appl. Therm. Eng.* **2018**, *139*, 387–394. [[CrossRef](#)]
31. Salaudeen, S.A.; Arku, P.; Dutta, A. *Gasification of Plastic Solid Waste and Competitive Technologies*; Elsevier Inc.: Amsterdam, The Netherlands, 2018; ISBN 9780128131404.
32. Jiang, K.; Cheng, C.; Ran, M.; Lu, Y.; Wu, Q. Preparation of a biochar with a high calorific value from chestnut shells. *New Carbon Mater.* **2018**, *33*, 183–187. [[CrossRef](#)]
33. Dabai, F.; Paterson, N.; Millan, M.; Fennell, P.; Kandiyoti, R. Tar formation and destruction in a fixed-bed reactor simulating downdraft gasification: Equipment development and characterization of tar-cracking products. *Energy Fuels* **2010**, *24*, 4560–4570. [[CrossRef](#)]
34. Viana, H.; Rodrigues, A.; Lopes, D.M.M.; Godina, R.; Nunes, L.J.R.; Matias, J.C.O. Pinus Pinaster and Eucalyptus Globulus Energetic Properties and Ash Characterization. In Proceedings of the 2018 IEEE International Conference on Environment and Electrical Engineering and 2018 IEEE Industrial and Commercial Power Systems Europe (EEEIC/I&CPS Europe), Palermo, Italy, 12–15 June 2018; pp. 1–4.
35. Pio, D.T.; Tarelho, L.A.C.; Tavares, A.M.A.; Matos, M.A.A.; Silva, V. Co-gasification of refused derived fuel and biomass in a pilot-scale bubbling fluidized bed reactor. *Energy Convers. Manag.* **2020**, *206*. [[CrossRef](#)]
36. Miranda, M.; Gulyurtlu, I.; Cabrita, I.; Pinto, F.; Franco, C.; Andre, R.N. Co-gasification study of biomass mixed with plastic wastes. *Fuel* **2002**, *81*, 291–297.
37. Ahmed, I.I.; Gupta, A.K. Kinetics of woodchips char gasification with steam and carbon dioxide. *Appl. Energy* **2011**, *88*, 1613–1619. [[CrossRef](#)]
38. van den Bergh, A. The Co-Gasification of Wood and Polyethylene the Influence of Temperature, Equivalence Ratio, Steam and the Feedstock Composition on the Gas Yield and Composition. Master's Thesis, Eindhoven University of Technology, Eindhoven, The Netherlands, 2005.
39. Kannan, P.; Al Shoaibi, A.; Srinivasakannan, C. Optimization of Waste Plastics Gasification Process Using Aspen-Plus. In *Gasification for Practical Applications*; Scitus Academics: Wilmington DE, USA, 2012.
40. Zeng, J.; Xiao, R.; Yuan, J. High-quality syngas production from biomass driven by chemical looping on a PY-GA coupled reactor. *Energy* **2021**, *214*, 118846. [[CrossRef](#)]
41. Innovative, O.; Recycling, P. Co-gasification of wood and polyethylene with the aim of CO and H<sub>2</sub> production. *J. Mater. Cycles Waste Manag.* **2006**, 95–98.
42. El-Hendawy, A.-N.A. Surface and adsorptive properties of carbons prepared from biomass. *Appl. Surf. Sci.* **2005**, *252*, 287–295. [[CrossRef](#)]
43. El-Hendawy, A.N.A. Variation in the FTIR spectra of a biomass under impregnation, carbonization and oxidation conditions. *J. Anal. Appl. Pyrolysis* **2006**, *75*, 159–166. [[CrossRef](#)]
44. Kiln, R.; Biomass, T.A. The concept, design and performance of a novel rotary kiln type air-staged biomass gasifier. *Energies* **2016**, *9*, 67.
45. Rahman, A.; Sudarmanta, B.; Fansuri, H.; Muraza, O. Syngas production from municipal solid waste with a reduced tar yield by three-stages of air inlet to a downdraft gasifier. *Fuel* **2020**, *263*, 116509.

46. Bhoi, P.R.; Huhnke, R.L.; Kumar, A.; Indrawan, N. Co-gasification of municipal solid waste and biomass in a commercial scale downdraft gasifier. *Energy* **2018**, *163*, 513–518. [[CrossRef](#)]
47. Patel, V.R.; Upadhyay, D.S.; Patel, R.N. Gasification of lignite in a fixed bed reactor: Influence of particle size on performance of downdraft gasifier. *Energy* **2014**, *78*, 323–332. [[CrossRef](#)]
48. Aznar, P.; Caballero, M.A.; Sancho, J.A.; Francés, E. Plastic waste elimination by co-gasification with coal and biomass in fluidized bed with air in pilot plant. *Fuel Process. Technol.* **2006**, *87*, 409–420. [[CrossRef](#)]
49. Kim, J.; Mun, T.; Kim, J.; Kim, J. Air gasification of mixed plastic wastes using a two-stage gasifier for the production of producer gas with low tar and a high caloric value. *Fuel* **2011**, *90*, 2266–2272. [[CrossRef](#)]
50. Toledo, J.M.; Aznar, M.P.; Sancho, J.A. Catalytic Air Gasification of Plastic Waste (Polypropylene) in a Fluidized Bed. Part II: Effects of Some Operating Variables on the Quality of the Raw Gas Produced Using Olivine as the In-Bed Material. *Ind. Eng. Chem. Res.* **2011**, *50*, 11815–11821. [[CrossRef](#)]
51. Cho, M.; Mun, T.; Kim, J. Air gasification of mixed plastic wastes using calcined dolomite and activated carbon in a two-stage gasifier to reduce tar. *Energy* **2013**, *53*, 299–305. [[CrossRef](#)]
52. Xiao, R.; Jin, B.; Zhou, H.; Zhong, Z.; Zhang, M. Air gasification of polypropylene plastic waste in fluidized bed gasifier. *Energy Convers. Manag.* **2007**, *48*, 778–786. [[CrossRef](#)]
53. Raman, P.; Ram, N.K. Performance analysis of an internal combustion engine operated on producer gas, in comparison with the performance of the natural gas and diesel engines. *Energy* **2013**, *63*, 317–333. [[CrossRef](#)]

**Publisher’s Note:** MDPI stays neutral with regard to jurisdictional claims in published maps and institutional affiliations.



© 2020 by the authors. Licensee MDPI, Basel, Switzerland. This article is an open access article distributed under the terms and conditions of the Creative Commons Attribution (CC BY) license (<http://creativecommons.org/licenses/by/4.0/>).